

## *ab initio* Structural, Electronic and Vibrational Properties of GaSb Nanocrystals Using Diamondoids and Large Unit Cell Method

MUDAR AHMED ABDULSATTAR<sup>1,\*</sup> and MAJED M. MOHAMAD<sup>2</sup>

<sup>1</sup>Ministry of Science and Technology, Baghdad, Iraq

<sup>2</sup>Higher Academy of Scientific and Human Studies, Baghdad, Iraq

\*Corresponding author: E-mail: mudarahmed3@yahoo.com

Received: 31 May 2014;

Accepted: 6 August 2014;

Published online: 17 March 2015;

AJC-16993

GaSb diamondoids and large unit cell method are used as building blocks to investigate size dependence of electronic properties of GaSb nanocrystals. Density functional theory is used combined with large unit cell and diamondoids structures. GaSbH<sub>6</sub> and Ga<sub>3</sub>Sb<sub>3</sub>H<sub>12</sub> molecules and GaSb diamondoids that include GaSb-diamantane, GaSb-tetramantane and GaSb-hexamantane are investigated in addition to 8, 16, 54 and 64 atoms large unit cells. Results show that energy gap generally decreases with shape fluctuations as the number of atoms increases and eventually stabilizes and gradually increases for the number of atoms greater than 200 atoms. Bond lengths and tetrahedral angles of diamondoids show that these molecules are very close to ideal zinc blende structure. Bond lengths encounter an expansion near the surface of diamondoids. Variation with size of some of the vibrational lines that include the radial breathing mode, highest force constant mode, Ga-H symmetric vibrations and Sb-H asymmetric vibrations is shown. A comparison with experiment reveals the good results that can be obtained from present theory.

**Keywords:** GaSb nanocrystals, Diamondoids, Structural, Unit cell method.

### INTRODUCTION

GaSb nanostructures had gained a lot of interest in recent applications. This includes nanowire field-effect transistors (NWFETs)<sup>1,2</sup>, quantum ring solar cells<sup>3</sup>, quantum cascade lasers<sup>4</sup>...*etc.* Heterojunctions of GaSb nanostructures with other semiconductors such as InAs are also widely investigated<sup>5</sup>. Some aspects of the superior performance of GaSb devices are at least proved theoretically<sup>1</sup>. Theoretical simulation of GaSb nanostructures or its heterostructures span the methods used previously for bulk calculations. This includes k.p method<sup>5,6</sup> and empirical pseudopotential method<sup>7,8</sup>. Since both Ga and Sb are heavy elements, their relativistic effects on GaSb band structure are also important<sup>9</sup>. The small gap of bulk GaSb (0.72 eV) makes it a good choice for infrared instrumentation<sup>3</sup>.

We shall deviate from the usual trend of methods for GaSb in the present work. Recent developments in nanocrystals calculations incorporate new methods such as the present two methods for the small and medium sizes of these nanocrystals<sup>10,11</sup>. For small nanocrystals and/or light elements the best method is cluster calculation that incorporates full geometrical optimization to minimize the total energy of the cluster. For larger nanocrystals that contain heavy elements the large unit cell (LUC) method is used<sup>10-12</sup> which is some kind of size-

limited supercell method that deviates from the original method that was used for bulk calculations<sup>12</sup>. These two methods can be compared with the k.p and empirical pseudopotential methods that are still used for larger nanocrystals or bulk. The reason for incorporating present cluster or LUC methods is that they use molecular bottom-up building of nanomaterials that give us additional understanding of how these materials are constructed. Diamondoids that are usually used as building blocks for diamond nanocrystals will be used for the first time in present work as building blocks of zinc blende GaSb nanocrystals. The same is true for the LUC method which has not been used for the present compound before. The LUC method is built from primitive or Bravais cells which are the smallest convenient units of a single lattice point of a structure with translational symmetry<sup>10-12</sup>.

### THEORY

In the present work, we shall use both cluster method and LUC method to investigate the electronic structure of GaSb nanocrystals of less than 3 nm in length. The cluster method simulates all of the nanocrystal including core and surface parts while the LUC method simulates the core part only of bigger size nanocrystals<sup>10,11</sup>. Density functional theory (DFT)

at the generalized gradient approximation level of Perdew, Burke and Ernzerhof (PBE) is used. PBE/3-21G method and basis are used whenever it is computationally appropriate or feasible (computational time or resources). STO-3G is used for large number of atoms particularly for LUC method calculations. Note that better basis sets such as 6-31G are not available for heavy elements such as Sb in Gaussian program. Ga and Sb are both heavy elements and contain large number of electrons and orbitals. This makes it difficult to use DFT theory in cluster form with large number of atoms that have no geometrical symmetry. Relativistic effects are taken into account by including estimated spin-orbit splitting to the value of the energy gap<sup>12</sup>. Clusters of GaSb include GaSbH<sub>6</sub>, Ga<sub>3</sub>Sb<sub>3</sub>H<sub>12</sub>, GaSb-diamantane (Ga<sub>7</sub>Sb<sub>7</sub>H<sub>20</sub>), GaSb-tetramantane [121] (Ga<sub>11</sub>Sb<sub>11</sub>H<sub>28</sub>), GaSb-tetramantane [123] (Ga<sub>11</sub>Sb<sub>11</sub>H<sub>28</sub>) and GaSb-hexamantane [12312] (Ga<sub>13</sub>Sb<sub>13</sub>H<sub>30</sub>). Fig. 1 shows diamondoids clusters.

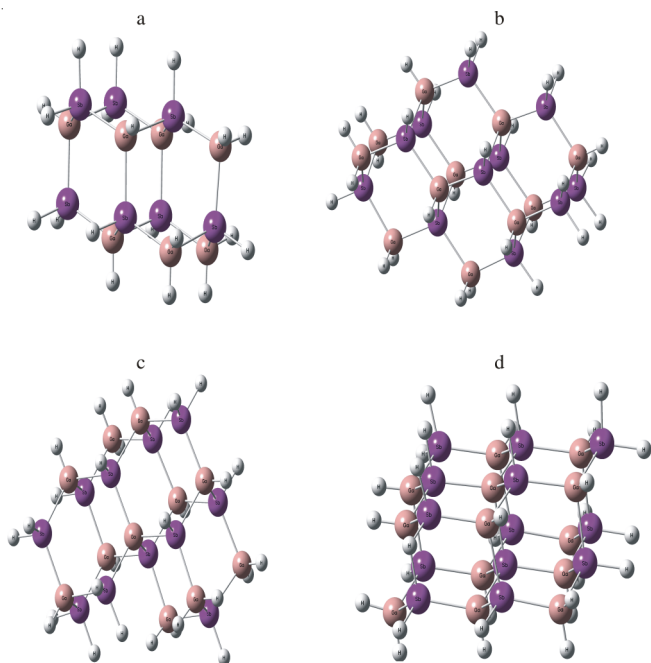


Fig. 1. Cluster shapes of geometrically optimized (a) GaSb-diamantane, (b) GaSb-tetramantane [121] (c) GaSb-tetramantane [123] (d) GaSb-hexamantane [12312]

The LUC method is a supercell method that repeats a central cell so that it corresponds to a limited periodical lattice that simulates the core part of a nanocrystal<sup>13</sup>. The calculations are performed for 8, 16, 54 and 64 atom LUCs that corresponds to 216, 325, 470 and 512 combined Ga and Sb atoms including the repeated cells<sup>14</sup>. These cells need to be optimized by optimizing their lattice constant only<sup>14</sup>. Fig. 2 shows that the 64 atom LUC. Both 8 and 64 LUCs are cubic Bravais cells while 16 and 54 cells are parallelepiped primitive cells. For more discussion on the methodology of LUC for nanocrystals we refer the reader to LUC nanocrystals literature<sup>10-14</sup>. Density functional theory calculations are performed using Gaussian03 program<sup>15</sup>. Symmetry is an important factor in quantum computing. Without symmetry the advanced methods such as DFT method face convergence problems as described in Gaussian03 program manual<sup>15</sup>. For the same reason we are

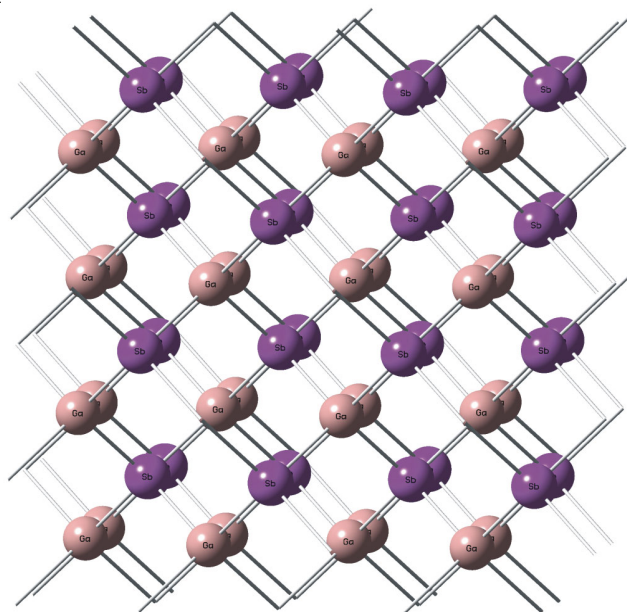


Fig. 2. 64 atom LUC (Ga<sub>32</sub>Sb<sub>32</sub>) that represents the core of 512 combined Ga and Sb atoms cluster (after adding the repeated cells)

able to reach high number of atoms in LUC method since we use the ideal zinc blende fully symmetric structure that does not need to go through full geometrical optimization.

## RESULTS AND DISCUSSION

Fig. 3 shows DFT calculated energy gaps (spin-orbit corrected) using both cluster (C-DFT) and large unit cell (LUC-DFT) methods. These energy gaps are compared with experimental bulk gap value 0.72 eV<sup>16</sup>. In this figure it is noted that the general dropping of the energy gap from nearly 5 eV in GaSb small molecules (GaSbH<sub>6</sub>, Ga<sub>3</sub>Sb<sub>3</sub>H<sub>12</sub>) until it nearly stabilizes at 1.5-1.7 eV at high number of atoms using LUC-DFT/STO-3G method and basis. The use of the more elaborate 3-21G double-zeta basis ends at 0.435 eV. This value is comparable to the experimental value 0.72 eV. This gap is expected to rise parallel to its STO-3G analogue to be very close to the bulk experimental value (Fig. 3). The gap is fluctuating at the beginning due to the change of shape of clusters and molecules. This change becomes less dramatic or important at high number of atoms and consequently less gap fluctuations. This behaviour is consistent with confinement and shape effects<sup>10-12</sup>. Figs. 1 and 2 illustrate the differences in geometry between the two methods used in the present work<sup>10,11,17</sup>.

Even-numbered diamondoids are used in Fig. 3 to show size and shape dependence of GaSb nanocrystals gap at the molecular limit of nanocrystals. Odd-numbered diamondoids (such as adamantane and triamantane) are not considered since they might have unequal number of Ga and Sb atoms. Diamondoids differ from other molecules mainly by their cage like structure and that their surface atoms are saturated by one or two hydrogen atoms only<sup>18</sup>. They were suggested and found experimentally for group IV elements in their diamond structure and can be used to investigate the variation of their corresponding nanocrystals properties<sup>19,20</sup>. In the present work we suggest to use these structures for III-V compounds. The reason for such suggestion is that III and V elements have +3 and +5

oxidation states in their compounds which make them stable in diamondoids structure even more than IV elements that have +4 oxidation states. The size variation is obvious from Fig. 3. Shape variation can also be seen by noting that the gap of the two isomers GaSb-tetramantane [121] and GaSb-tetramantane [123] are 1.8 and 2.4 eV, respectively using PBE/3-21G method. The high symmetry and stability of presently suggested GaSb-diamondoid structures make them candidates for further future experimental and theoretical exploration.

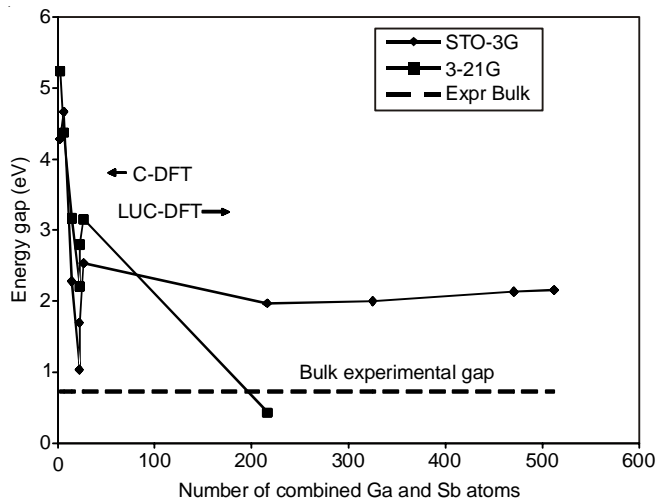


Fig. 3. Energy gap (spin-orbit corrected) as a function of number of core atoms for GaSb nanocrystals and molecules. The dashed line represents the experimental value of bulk GaSb gap at 0.72 eV [Ref. 16,18]

Fig. 4 illustrates Ga-Sb bond lengths as a function of number of atoms for GaSb diamondoids and nanocrystals. The figure shows that PBE/3-21G method has a decreasing Ga-Sb bond length which is what we expect experimentally. The LUC results using 3-21G basis gives a higher bond length at 2.71 Å. On the other hand Ga-Sb bond lengths using PBE/STO-3G show oscillating behaviour that stabilize at 2.42 Å. The reason for performing PBE/STO-3G calculations is to obtain the results for higher number of atoms that can not be performed using the superior PBE/3-21G method. Ga-Sb bond length is compared with experimental bulk value of 2.64 Å<sup>16</sup>. From Fig. 4 we expect that Ga-Sb bond length converges near the experimental bond length for the high number of atoms using PBE/3-21G method provided that 3-21G results continues to be parallel to its STO-3G counterpart. LUC calculations using 3-21G basis on the other hand show that smaller nanocrystals experience an expansion in their bond length. This expansion is consistent with experimental and previous LUC results<sup>13,14,17</sup>. A comparison of performance of PBE/STO-3G and PBE/3-21G methods on different molecules can be found in reference<sup>21</sup>.

Fig. 5 illustrates bonds length as a function of number of layer for GaSb-hexamantane that connects two opposite corners of this molecule using PBE/3-21G method. At the two ends H-Sb and Ga-H bond lengths have the values 1.76 and 1.58 Å, respectively. These bond lengths are nearly constant for all other diamondoids since these bonds exist only at the surface. The Ga-Sb bond decreases as we go to the center of the molecule. The value of this bond at the center nearly coincides with the bulk experimental value.

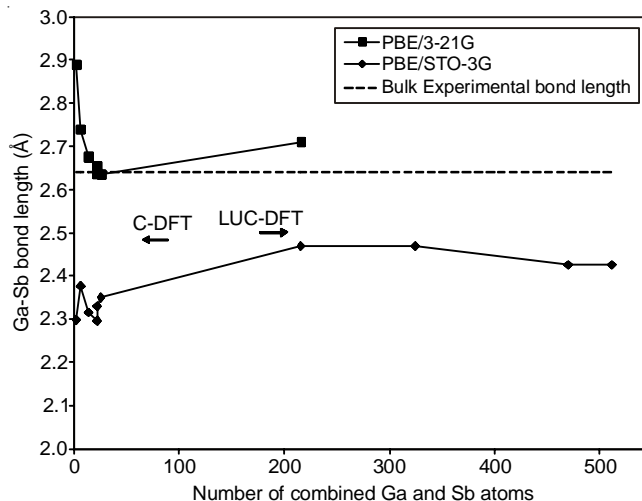


Fig. 4. Ga-Sb bond lengths as a function of number of atoms for GaSb diamondoids and nanocrystals. The dashed line represents the Ga-Sb experimental bulk value of bond length [Ref.17]

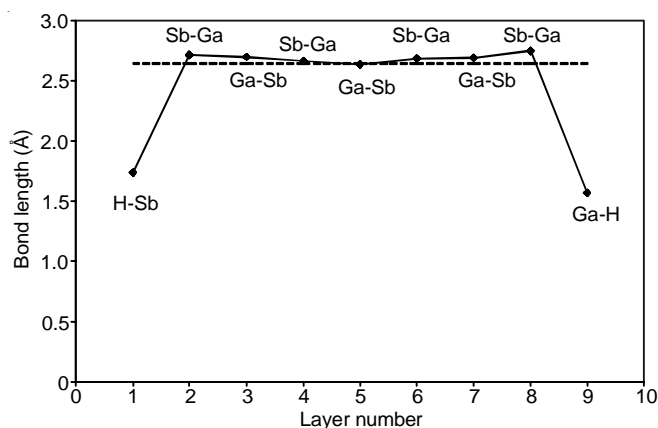


Fig. 5. Bonds length as a function of number of layer for GaSb-hexamantane that connects two opposite corners using PBE/3-21G method. The dashed line represents the experimental bulk value of bond length [Ref. 16]

Fig. 6 shows tetrahedral angles as a function of number of layer for GaSb hexamantane using the same trajectory that connects two opposite corners in Fig. 5. This figure shows that this angle is confined between narrow limits (105.5 to 116.2 degrees) around the ideal value of 109.47<sup>11</sup>. The values of these angles are closer to the ideal value at the center and boundary of the molecule for two different reasons. At the center of the molecule the structure is approaching the ideal zinc-blende structure. At the boundaries H atoms are restricted in their movement at one side only and free to move at the other side. This one-sided freedom gives the atom the opportunity to occupy a more close location to the ideal position.

Figs. 7 to 9 illustrate density of states of the various sizes and methods used in the present work. Density of states can be used to determine energy gap, width of valence and conduction bands, the position of highest occupied molecular orbital (HOMO), lowest unoccupied molecular orbital (LUMO) and the Fermi level. Energy range in these figures is kept from -30 to 30 eV for comparison.

Fig. 7 shows density of states of GaSb 54 atom LUC as a function of levels energy. Comparing this figure with Fig. 8 for the 64 atom LUC reveals several differences. The first

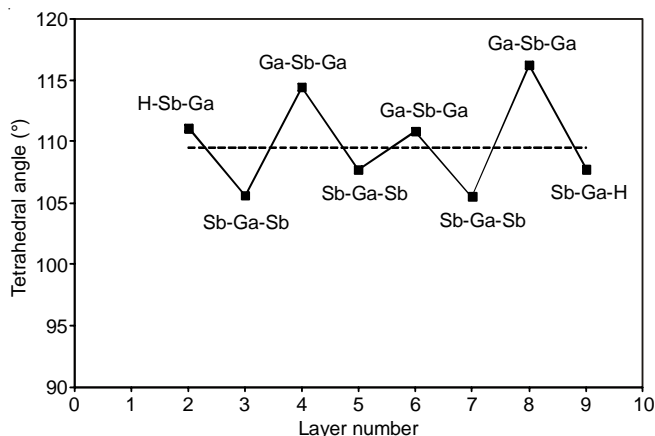


Fig. 6. Tetrahedral angles (in degrees) as a function of number of layer for GaSb hexamantane using the same trajectory that connects two opposite corners in Fig. 5. The calculations are performed using PBE/3-21G method. The dashed line represents the ideal bulk value of the tetrahedral angle of zinc-blende and diamond structures at  $109.47^\circ$  [Ref. 11]

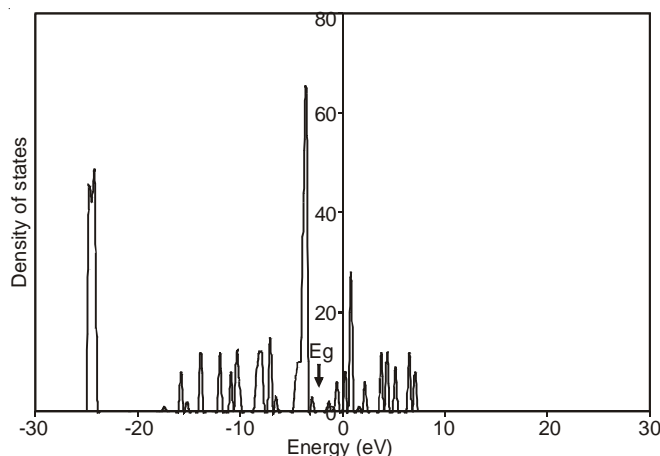


Fig. 7. Density of states of GaSb 54 atoms LUC as a function of levels energy

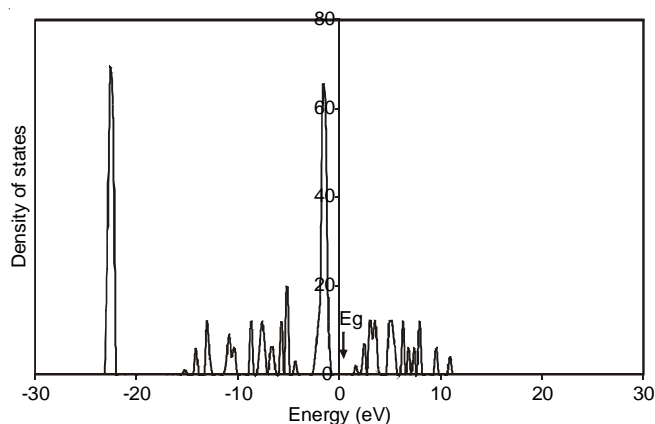


Fig. 8. Density of states of GaSb 64 atoms LUC as a function of levels energy

difference is the movement of density of states of 64 atoms LUC to the direction of a more positive energy values with respect to the 54 atoms LUC. The second difference is the change of heights and positions of several peaks between the two figures. Both of these differences are due to the differences between cell shapes and consequently Brillion zones and band structures. These changes between cells were pointed before in previous LUC calculations<sup>13</sup>.

Density of state in Fig. 9 differ from that of Figs. 7,8 in that they include the complete surface and core of GaSb-hexamantane molecule or nanocrystal while Figs.7,8 (LUC method) include only the ideal structure of the core part (without the surface). Fig. 9 also has very wider conduction band due to the addition of surface states. Density of state in Fig. 9 has less sharp peaks due to surface atoms effect that strain the nanocrystals bonds and consequently reduces the degeneracy of states and their sharpness. The position of the gap in GaSb-hexamantane is very near of that of 54 atom LUC. This shows that diamondoids are similar to primitive cells rather than Bravais cells in shape and other properties.

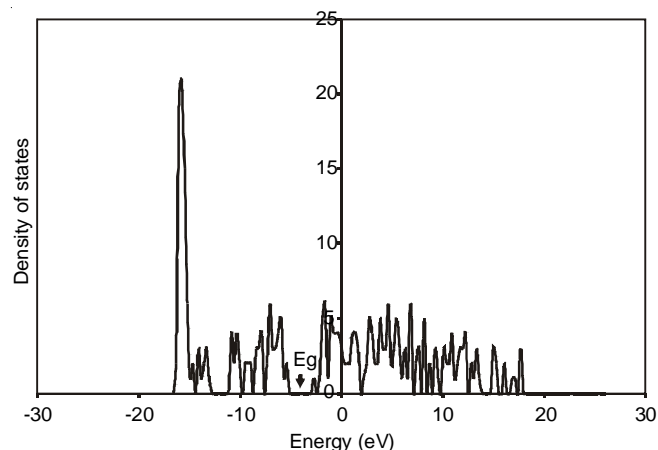


Fig. 9. Density of states of GaSb-hexamantane molecule as a function of levels energy

In Fig. 10, the variation of some of the vibrational lines (infrared and Raman) are shown. These include the radial breathing mode (RBM), highest force constant mode in the optical branch (HFCM), Ga-H symmetric vibrations and Sb-H asymmetric vibrations. These vibrations are chosen because of the following reasons:

The radial breathing mode converges to  $0 \text{ cm}^{-1}$  for bulk materials<sup>17</sup>. As a result it is usually one of the lowest vibrations that the Raman and IR spectral vibrations start with (very near to  $0 \text{ cm}^{-1}$ ). The convergence to  $0 \text{ cm}^{-1}$  for large number of atoms is shown in Fig. 10. The highest force constant mode in branch in the optical branch of vibrations is shown previously to converge to the longitudinal optical mode (LO) for the case of carbon and silicon<sup>19,20</sup>. The present case for GaSb diamondoids also follows the same trend of convergence to LO mode as shown in Fig. 10. The IR and Raman vibrational spectra of surface hydrogenated materials usually contain two parts that are separated by a frequency gap. The first part contains heavy atom vibrations plus some hydrogen vibrations. The second vibrational part is characterized by symmetric and asymmetric hydrogen atom vibrations only. In the present case the second part is bounded by Ga-H symmetric vibrations and Sb-H asymmetric vibrations respectively as shown in Fig. 10. Unlike radial breathing mode and highest force constant mode in branch the symmetric and asymmetric hydrogen vibrations are nearly constant and does not change appreciably with nanoparticle size variation in analogues to H bond lengths (Fig. 5).

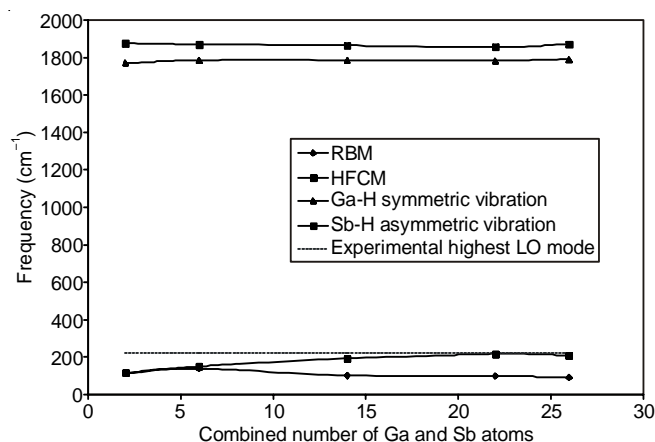


Fig. 10. Variation of radial breathing mode (RBM), highest force constant mode in the optical branch (HFCM), Ga-H symmetric vibrations and Sb-H asymmetric vibrations is shown

### Conclusion

Diamonoids and LUC method are suggested in the present work to be building blocks of GaSb nanocrystals. The structure of these building blocks is proved to be stable using DFT theory. Diamonoids and LUC size and shape variation show their effect on the variation of the energy gap and bond lengths. GaSb surfaces play an important role on the density of states, bond lengths, tetrahedral angles, *etc.* of these molecules or nanocrystals. Effect of surfaces can be recognized when we compare LUC results (which are surface free calculations) with that of cluster of atoms calculations. Density of states is sharper and higher at the center of the nanocrystal using LUC method. These states are less sharp and melt down at the surface due to surface discontinuity, passivating atoms and surface reconstruction. The variation of vibrational lines show the expected trends of radial breathing mode, highest force constant mode, Ga-H symmetric and Sb-H asymmetric vibrations.

### REFERENCES

1. K. Shimoida, H. Tsuchiya, Y. Kamakura, N. Mori and M. Ogawa, *Appl. Phys. Express*, **6**, 034301 (2013).
2. A.W. Dey, B.M. Borg, B. Ganjipour, M. Ek, K.A. Dick, E. Lind, C. Thelander and L.E. Wernersson, *IEEE Electron Device Lett.*, **34**, 211 (2013).
3. P.J. Carrington, M.C. Wagener, J.R. Botha, A.M. Sanchez and A. Krier, *Appl. Phys. Lett.*, **101**, 231101 (2012).
4. Y.H. Ko, B.D. Park and J.S. Yu, *J. Korean Phys. Soc.*, **61**, 1365 (2012).
5. V.V.R. Kishore, B. Partoens and F.M. Peeters, *Phys. Rev. B*, **86**, 165439 (2012).
6. A.J. Martin, J. Hwang, E.A. Marquis, E. Smakman, T.W. Saucer, G.V. Rodriguez, A.H. Hunter, V. Sih, P.M. Koenraad, J.D. Phillips and J. Millunchick, *Appl. Phys. Lett.*, **102**, 113103 (2013).
7. N. Gautam, A. Barve and S. Krishna, *Appl. Phys. Lett.*, **101**, 221119 (2012).
8. W.F. Sun, *Acta Phys. Sin.*, **61**, 117104 (2012).
9. A. Zakharova, I. Semenikhin and K.A. Chao, *JETP Lett.*, **94**, 660 (2011).
10. H.R. Jappor, Z.A. Saleh and M.A. Abdulsattar, *Adv. Mater. Sci. Eng.*, **2012**, 1 (2012).
11. H.N. Nasir, M.A. Abdulsattar and H.M. Abduljalil, *Adv. Condens. Matter Phys.*, Article ID 348254 (2012).
12. M.A. Abdulsattar and K.H. Al-Bayati, *Phys. Rev. B*, **75**, 245201 (2007).
13. H.M. Abduljalil, M.A. Abdulsattar and S.R. Al-Mansoury, *Micro & Nano Lett.*, **6**, 386 (2011).
14. M.A. Abdulsattar, *Solid State Sci.*, **13**, 843 (2011).
15. Gaussian 03, Revision B.01; Gaussian, Inc.: C.T. Wallingford, USA (2003).
16. T.-C. Chiang and D.E. Eastman, *Phys. Rev. B*, **22**, 2940 (1980).
17. C. Kittel, *Introduction to Solid State Physics*, Wiley, edn. 8 (2005).
18. L. Landt, K. Klünder, J.E. Dahl, R.M.K. Carlson, T. Möller and C. Bostedt, *Phys. Rev. Lett.*, **103**, 047402 (2009).
19. M.A. Abdulsattar, *Beilstein J. Nanotechnol.*, **4**, 262 (2013).
20. M.A. Abdulsattar, *Silicon*, **5**, 229 (2013).
21. NIST Computational Chemistry Comparison and Benchmark Database, Release 15b, 2011. <http://cccbdb.nist.gov/> (Accessed Jun. 1, 2013).